Development of a Pressure-Dependent Constitutive Model with Combined Multilinear Kinematic and Isotropic Hardening

Phillip A. Allen* and Christopher D. Wilson†

*Strength Analysis Group / ED22, NASA MSFC, phillip.a.allen@nasa.gov

†Dept. of Mechanical Engineering, Tennessee Technological University, chriswilson@tntech.edu

Abstract: The development of a pressure-dependent constitutive model with combined multilinear kinematic and isotropic hardening is presented. The constitutive model is developed using the ABAQUS user material subroutine (UMAT). First the pressure-dependent plasticity model is derived. Following this, the combined bilinear and combined multilinear hardening equations are developed for von Mises plasticity theory. The hardening rule equations are then modified to include pressure dependency. The method for implementing the new constitutive model into ABAQUS is given. Finally, verification of the UMAT is presented.

Keywords: Combined Multilinear Hardening, Drucker-Prager, Hydrostatic Stress, Isotropic Hardening, Kinematic Hardening, Low Cycle Fatigue, Plasticity, Pressure-Dependent, UMAT.

1. Introduction

Classical metal plasticity theory assumes that hydrostatic stress has a negligible effect on the yield behavior of metals (Bridgman, 1947; Hill, 1950). Spitzig (1975, 1976,1984) and Richmond (1980) conducted experiments demonstrating that yielding in metals could be approximated as a linear function of hydrostatic stress. Recent reexaminations of classical theory by Wilson (2002) and Allen (2000,2002) have revealed a significant effect of hydrostatic stress on the yield behavior of various metals. An ABAQUS user material subroutine (UMAT) was developed to investigate the effect of hydrostatic stress on low cycle fatigue of metals. The UMAT is based on the Drucker-Prager (1952) yield theory and incorporates combined multilinear kinematic and isotropic hardening. A summary of the development of the UMAT is presented here. See Allen (2002) for more details on the UMAT development including the corresponding UMAT FORTRAN code.

2. Pressure-dependent plasticity model

This section details the development of the governing equations for a pressure-dependent plasticity model including numerical methods for the integration of the constitutive equations. The equations are derived using the method developed by Aravas (1987,1996). The tensor components are given with respect to a cartesian coordinate system with indices ranging from 1 to 3.

2.1 Yield function

The chosen pressure-dependent yield function is the Drucker-Prager yield function. The Drucker-Prager yield function is written in ABAQUS (ABAQUS, 1995) notation as

$$f = t - p\tan\theta - d = 0, \tag{1}$$

where t is a pseudo-effective stress , θ is the slope of the linear yield surface in the p-t stress plane, p is the hydrostatic pressure, d is the effective cohesion of the material. In metal plasticity, d is equivalent to the current yield stress, σ_{ys}. In general, σ_{ys} is a function of the equivalent plastic strain, ε_{eq}^{pl} , which is given by the equation

$$\varepsilon_{eq}^{pl} = \sqrt{\frac{2}{3}\varepsilon_{ij}^{pl}\varepsilon_{ij}^{pl}}\ , \tag{2}$$

where ε_{ij}^{pl} is the plastic strain ($\varepsilon_{ij}^{pl} = \varepsilon_{ij} - \varepsilon_{ij}^{el}$).

The variables used by the linear Drucker-Prager yield function are shown graphically in Figure 1.

The flow potential, g, for the linear Drucker-Prager model is defined as

$$g = t - p\tan\psi, \tag{3}$$

where ψ is the dilation angle in the p-t plane. Setting $\psi = \theta$ results in associated flow. Therefore, the original Drucker-Prager model is available by setting $\psi = \theta$ and $r = 1$, which leads to $t = \sqrt{3J_2}$. Substituting $p = -\frac{1}{3}I_1$ into equation (1) gives

$$f = \sqrt{3J_2} + \frac{1}{3}I_1\tan\theta - d, \tag{4}$$

where I_1 is the first stress invariant. To conveniently compare ABAQUS Drucker-Prager material property variables with those used by Richmond, *et al.* (1980) in their material testing let

$$a = \frac{1}{3}\tan\theta. \tag{5}$$

Finally, Equation (4) can be written as

$$f = \sigma_{eff} - 3ap - \sigma_{ys}\left(\varepsilon_{eq}^{pl}\right) = 0\,, \tag{6}$$

where σ_{eff} is the effective stress for von Mises plasticity theory.

2.2 Flow Rule

The rate form of the associated flow rule is written as

$$\dot{\varepsilon}_{ij}^{pl} = \dot{\phi}\frac{\partial f}{\partial \sigma_{ij}}\,. \tag{7}$$

The flow rule is written in a more general form as

$$\dot{\varepsilon}_{ij}^{pl} = \dot{\varepsilon}_q \bar{n}_{ij} + \frac{1}{3}\dot{\varepsilon}_p \bar{\mathrm{I}}\,, \tag{8}$$

where

$$\bar{n}_{ij} = \frac{3}{2}\frac{S_{ij}}{\sigma_{eff}}\,, \tag{9}$$

$$\dot{\varepsilon}_q = \dot{\phi}\frac{\partial f}{\partial \sigma_{eff}}\,, \tag{10}$$

$$\dot{\varepsilon}_p = -\dot{\phi}\frac{\partial f}{\partial p}\,, \tag{11}$$

where S_{ij} is the deviatoric stress tensor and $\dot{\varepsilon}_q$ and $\dot{\varepsilon}_p$ are the distortional and volumetric portions of the plastic strain rate, respectively. Eliminating $\dot{\phi}$ from Equations (10) and (11) gives

$$\dot{\varepsilon}_q \frac{\partial f}{\partial p} + \dot{\varepsilon}_p \frac{\partial f}{\partial \sigma_{eff}} = 0\,, \tag{12}$$

and Equation (12) can be rewritten as

$$\dot{\varepsilon}_q\left(-3a\right) + \dot{\varepsilon}_p = 0\,. \tag{13}$$

2.3 State variable equations

For the case of the linear Drucker-Prager model, only one state variable, $\dot{\Gamma}^1$ is required and is defined as

$$\dot{\Gamma}^1 \equiv \dot{\varepsilon}_{eq}^{pl}\,. \tag{14}$$

The plastic work equation is used to derive a usable form of the state variable equation, which can be written as

$$\dot{\varepsilon}_{eq}^{pl} = \frac{-p\dot{\varepsilon}_p + \sigma_{eff}\dot{\varepsilon}_q}{\sigma_{ys}\left(\varepsilon_{eq}^{pl}\right)}. \tag{15}$$

2.4 Numerical integration

The backward (implicit) Euler method was chosen for the integration of the elastoplastic equations. Ortiz and Popov (1985) found that the backward Euler method is very accurate for strain increments several times the size of the yield surface in strain space and that the method is unconditionally stable.

Assuming isotropic linear elasticity, one can write

$$\sigma_{ij} = 2\mu\varepsilon_{ij}^{el} + K\varepsilon_{kk}^{el}\bar{\mathrm{I}}_{ij}, \tag{16}$$

where σ_{ij} is the stress tensor, μ is the shear modulus, K is the bulk modulus, and $\bar{\mathrm{I}}_{ij}$ is the second-order identity tensor. Using the backward Euler method to integrate equations (16), (8), (13) and (15) leads to the following incremental forms

$$\sigma_{ij}\Big|_{n+1} = \sigma_{ij}^{pr} - 2\mu\Delta\varepsilon_q \bar{n}_{ij}\Big|_{n+1} - K\Delta\varepsilon_p\bar{\mathrm{I}}_{ij}, \tag{17}$$

$$\Delta\varepsilon_{ij}^{pl} = \Delta\varepsilon_q \bar{n}_{ij}\Big|_{n+1} + \frac{1}{3}\Delta\varepsilon_p\bar{\mathrm{I}}_{ij}, \tag{18}$$

$$\Delta\varepsilon_q(-3a) + \Delta\varepsilon_p = 0, \tag{19}$$

and

$$\Delta\varepsilon_{eq}^{pl} = \frac{-p\Delta\varepsilon_p + \sigma_{eff}\Delta\varepsilon_q}{\sigma_{ys}\left(\varepsilon_{eq}^{pl}\right)}. \tag{20}$$

The "n+1" subscript denotes values at the end of the increment at time, $t\big|_{n+1} = t\big|_n + \Delta t$, and the "pr" superscript indicates a predicted value based on the purely elastic solution.

Summarizing the primary equations and dropping the "n+1" subscript for brevity, one can write

$$f = \sigma_{eff} - 3ap - \sigma_{ys}\left(\varepsilon_{eq}^{pl}\right) = 0, \tag{21}$$

$$\Delta\varepsilon_q(-3a) + \Delta\varepsilon_p = 0, \tag{22}$$

$$(\sigma_{eff}) = \sigma_{eff}^{pr} - 3\mu\Delta\varepsilon_q, \tag{23}$$

$$p = p^{pr} + K\Delta\varepsilon_p, \tag{24}$$

and

$$\Delta\varepsilon_{eq}^{pl} = \frac{-p\Delta\varepsilon_p + \sigma_{eff}\Delta\varepsilon_q}{\sigma_{ys}\left(\varepsilon_{eq}^{pl}\right)}. \tag{25}$$

This forms a set of five nonlinear equations that is solved for p, σ_{eff}, $\Delta\varepsilon_p$, $\Delta\varepsilon_q$, and $\Delta\varepsilon_{eq}^{pl}$. Solving Equations (21) through (25) for the five unknowns gives

$$p = \frac{p^{pr}\mu + Ka\sigma_{eff}^{pr} - Ka\sigma_{ys}\left(\varepsilon_{eq}^{pl}\right)}{3Ka^2 + \mu}, \tag{26}$$

$$\sigma_{eff} = \frac{3ap^{pr}\mu + 3K\sigma_{eff}^{pr}a^2 + \mu\sigma_{ys}\left(\varepsilon_{eq}^{pl}\right)}{3Ka^2 + \mu}, \tag{27}$$

$$\Delta\varepsilon_p = \frac{a\left[\sigma_{eff}^{pr} - \sigma_{ys}\left(\varepsilon_{eq}^{pl}\right) - 3ap^{pr}\right]}{3Ka^2 + \mu}, \tag{28}$$

$$\Delta\varepsilon_q = \frac{\sigma_{eff}^{pr} - \sigma_{ys}\left(\varepsilon_{eq}^{pl}\right) - 3a\bar{p}^{pr}}{9Ka^2 + 3\mu}, \tag{29}$$

and

$$\Delta\varepsilon_{eq}^{pl} = \frac{\sigma_{eff}^{pr} - \sigma_{ys}\left(\varepsilon_{eq}^{pl}\right) - 3ap^{pr}}{9Ka^2 + 3\mu}. \tag{30}$$

In general, Newton iteration is used to solve Equation (30) for $\Delta\varepsilon_{eq}^{pl}$ and $\sigma_{ys}\left(\varepsilon_{eq}^{pl}\right)$, and then Equations (26) through (29) are solved by direct substitution. Strain increments and stresses are then determined by

$$\Delta\varepsilon_{ij}^{pl} = \frac{1}{3}\Delta\varepsilon_p\bar{\mathrm{I}}_{ij} + \Delta\varepsilon_q\bar{n}_{ij} \tag{31}$$

and

$$\sigma_{ij} = -p\bar{\mathrm{I}}_{ij} + \frac{2}{3}\sigma_{eff}\bar{n}_{ij} \tag{32}$$

thereby completing the solution of the elastoplastic equations.

In an implicit finite element code, such as ABAQUS, the equilibrium equations are written at the end of the increment resulting in a set of nonlinear equations in terms of the nodal unknowns. If a Newton scheme is used to solve the global nonlinear equations, the Jacobian (tangent stiffness) must be calculated (Aravas, 1996). The Jacobian, J is defined as

$$J = \frac{\partial\sigma\big|_{n+1}}{\partial\varepsilon\big|_{n+1}}. \tag{33}$$

The accuracy of Jacobian effects convergence, and, therefore, errors in the Jacobian formulation may result in analyses that require more iterations or, in some cases, diverge (ABAQUS, 2001). The Jacobian for von Mises plasticity was employed in this research.

3. Hardening models

Next, the development of the combined kinematic and isotropic hardening models is presented. For simplicity, the hardening equations for the classical von Mises theory along with a bilinear hardening theory are developed first. The derivation of the bilinear hardening equations closely parallels the work of Taylor and Flanagan (1998). These equations are then modified to form the more complex multilinear hardening equations. Finally, the bilinear and multilinear equations are modified to include the Drucker-Prager pressure dependency. To begin, several terms that are common to each of the hardening models are defined.

3.1 Basic definitions

The center of the yield surface in deviatoric stress space (the backstress) is defined by the tensor α_{ij}. The deviatoric stress tensor, S_{ij} is defined as

$$S_{ij} = \sigma_{ij} - \frac{1}{3} I_1 . \tag{34}$$

The stress difference, ξ_{ij} is defined by

$$\xi_{ij} = S_{ij} - \alpha_{ij} . \tag{35}$$

The magnitude of the stress difference, R, is then written as

$$R = \left| \xi_{ij} \right| = \sqrt{\xi_{ij} \xi_{ij}} . \tag{36}$$

The geometric relationship between ξ_{ij}, α_{ij}, and S_{ij} leads to taking the magnitude of the stress difference as a radius, hence the symbol R. The von Mises yield surface in terms of the stress difference is

$$f = \frac{1}{2} \xi_{ij} \xi_{ij} = k^2 , \tag{37}$$

where k is the yield strength in pure shear, and the effective stress is

$$\sigma_{eff} = \sqrt{\frac{3}{2} \xi_{ij} \xi_{ij}} . \tag{38}$$

Combining Equations (36) and (38), one defines R as

$$R = \sqrt{\frac{2}{3}} \sigma_{eff} . \tag{39}$$

The normal to the yield surface, Q_{ij} is then determined from Equation (37) as

$$Q_{ij} = \frac{\partial f / \partial \sigma_{ij}}{\left| \partial f / \partial \sigma_{ij} \right|} = \frac{\xi_{ij}}{R}. \tag{40}$$

Assuming a normality condition, the plastic part of the strain is

$$\varepsilon_{ij}^{pl} = \gamma Q_{ij}, \tag{41}$$

where γ is a scalar multiplier that must be determined (Taylor, 1998).

3.2 Combined bilinear hardening

Assuming a linear combination of the two hardening types, a scalar parameter, β, can be defined which determines the amount of each type of hardening with $0 \le \beta \le 1$. A value of $\beta = 1$ indicates only isotropic hardening, and a value of $\beta = 0$ indicates only kinematic hardening.

Equations for R and α_{ij} are written as

$$\dot{R} = \sqrt{\frac{2}{3}} H \dot{\varepsilon}_{eq}^{pl} \beta \tag{42}$$

and

$$\dot{\alpha}_{ij} = \frac{2}{3} H \gamma Q_{ij} (1 - \beta), \tag{43}$$

where H is the slope of the equivalent stress versus the equivalent plastic strain as shown in Figure 2. The consistency equation is formed as

$$Q_{ij} \dot{\xi}_{ij} = \dot{R} \tag{44}$$

or

$$Q_{ij} \left(\dot{S}_{ij} - \dot{\alpha}_{ij} \right) = \sqrt{\frac{2}{3}} H \dot{\varepsilon}_{eq}^{pl} \beta. \tag{45}$$

Using the additive strain rate decomposition and the elastic stress rate with Equation (45) and taking the tensor product with the normal, Q_{ij} gives

$$Q_{ij} \dot{\sigma}_{ij}^{pr} - \gamma Q_{ij} D_{ijkl} Q_{kl} - Q_{ij} \left[\frac{2}{3} H \gamma (1 - \beta) \right] Q_{ij} = Q_{ij} \left[\sqrt{\frac{2}{3}} H \sqrt{\frac{2}{3}} \beta \gamma \right] Q_{ij}. \tag{46}$$

Solving for γ gives

$$\gamma = \frac{1}{\left(1+\frac{H}{3\mu}\right)} Q_{ij}\varepsilon_{ij} \,. \tag{47}$$

The incremental forms of the governing equations are

$$\sigma_{ij}\Big|_{n+1} = \sigma_{ij}^{pr}\Big|_{n+1} - \Delta\gamma 2\mu Q_{ij}\,, \tag{48}$$

$$R\Big|_{n+1} = R\Big|_{n} + \frac{2}{3}H\Delta\gamma\beta\,, \tag{49}$$

and

$$\alpha_{ij}\Big|_{n+1} = \alpha_{ij}\Big|_{n} + \frac{2}{3}H\Delta\gamma Q_{ij}(1-\beta) \tag{50}$$

where, as before, the subscripts "n" and "n+1" refer to the beginning and end of a time step, respectively.

An incremental form of the consistency condition is also required and is written as

$$\alpha_{ij}\Big|_{n+1} + R\Big|_{n+1} Q_{ij} = S_{ij}\Big|_{n+1} \,. \tag{51}$$

Substituting Equations (48) through (50) into the consistency condition of (51) gives

$$\left[\alpha_{ij}\Big|_{n} + \frac{2}{3}H\Delta\gamma Q_{ij}(1-\beta)\right] + \left[R\Big|_{n} + \frac{2}{3}H\Delta\gamma\beta\right]Q_{ij} = S_{ij}^{pr}\Big|_{n+1} - \Delta\gamma 2\mu Q_{ij} \,. \tag{52}$$

Taking the tensor product of both sides of the previous equation with Q_{ij} and solving for $\Delta\gamma$ gives

$$\Delta\gamma = \frac{1}{2\mu\left(1+\frac{H}{3\mu}\right)}\left(\left|\xi_{ij}^{pr}\Big|_{n+1}\right| - R\Big|_{n}\right). \tag{53}$$

Equation (53) demonstrates that the plastic strain increment is proportional to the magnitude of the distance of the elastic predictor stress past the yield surface Having now determined $\Delta\gamma$ from Equation (53) Equations (48) through (50) can be solved. In addition, one also computes

$$\Delta\varepsilon_{il}^{pl} = Q_{ij}\Delta\gamma \tag{54}$$

and

$$\Delta\varepsilon_{eq}^{pl} = \sqrt{\frac{2}{3}}\,\Delta\gamma\,, \tag{55}$$

which completes the bilinear combined hardening incremental solution (Taylor, 1998).

3.3 Combined multilinear hardening

The equations for the multilinear hardening case are similar to those for the bilinear case, but an added level of complexity is required because the slope of the equivalent stress versus equivalent plastic strain, H is no longer constant. This complication is clearly seen by examining Figure 2, where for a given plastic strain increment, H may take on several values, H_i.

Recall that for bilinear hardening $\Delta\sigma_{eff}$ was written as

$$\Delta\sigma_{eff} = H\Delta\varepsilon_{eq}^{pl} = H\sqrt{\frac{2}{3}}\Delta\gamma\,. \tag{56}$$

Similarly, for the multilinear hardening case $\Delta\sigma_{eff}$ can be written as

$$\Delta\sigma_{eff} = h\left(\varepsilon_{eq}^{pl}\right)\Delta\varepsilon_{eq}^{pl} = h\left(\varepsilon_{eq}^{pl}\right)\sqrt{\frac{2}{3}}\Delta\gamma\,, \tag{57}$$

where $h\left(\varepsilon_{eq}^{pl}\right)$ is a hardening function. Substituting $h\left(\varepsilon_{eq}^{pl}\right)$ for H in Equations 42 and 43 and integrating gives

$$\Delta R = \beta\sqrt{\frac{2}{3}}\left[h\left(\varepsilon_{eq}^{pl}\Big|_n + \Delta\varepsilon_{eq}^{pl}\right) - h\left(\varepsilon_{eq}^{pl}\Big|_n\right)\right], \tag{58}$$

and

$$\Delta\alpha_{ij} = (1-\beta)\frac{2}{3}\left[h\left(\varepsilon_{eq}^{pl}\Big|_n + \Delta\varepsilon_{eq}^{pl}\right) - h\left(\varepsilon_{eq}^{pl}\Big|_n\right)\right]Q_{ij}\Big|_{n+1}\,. \tag{59}$$

Rewriting Equation (51) in terms of Equations (58) and (59) (where $R\big|_{n+1} = R\big|_n + \Delta R$, etc.) gives

$$S_{ij}^{pr} - \alpha_{ij}\Big|_n = \left\{2\mu\sqrt{\frac{3}{2}}\Delta\varepsilon_{eq}^{pl} + R\Big|_n + \sqrt{\frac{2}{3}}\left[h\left(\varepsilon_{eq}^{pl}\Big|_n + \Delta\varepsilon_{eq}^{pl}\right) - h\left(\varepsilon_{eq}^{pl}\Big|_n\right)\right]\right\}Q_{ij}\Big|_{n+1}\,. \tag{60}$$

Multiplying both sides of the previous equation by $Q_{ij}\big|_{n+1}$ leads to

$$2\mu\Delta\varepsilon_{eq}^{pl} + \frac{2}{3}\left[h\left(\varepsilon_{eq}^{pl}\Big|_n + \Delta\varepsilon_{eq}^{pl}\right) - h\left(\varepsilon_{eq}^{pl}\Big|_n\right)\right] = \sqrt{\frac{2}{3}}\left[\left\|S_{ij}^{pr} - \alpha_{ij}\Big|_n\right\| - R\Big|_n\right], \tag{61}$$

which is a nonlinear equation that can be solved for $\Delta\varepsilon_{eq}^{pl}$. Once $\Delta\varepsilon_{eq}^{pl}$ is known, the remaining incremental elastoplastic equations can be solved following the method demonstrated for the bilinear hardening case.

3.4 Pressure-dependent combined hardening

To conveniently compare the pressure-independent combined hardening equations with the previously derived Drucker-Prager elastoplastic equations, the following substitutions are made:

$$R\big|_n = \sqrt{\frac{2}{3}}\sigma_{ys}\big|_n, \tag{62}$$

$$\left|S_{ij}^{pr} - R\big|_n\right| = \left|\xi^{pr}\big|_{n+1}\right| = \sqrt{\frac{2}{3}}\sigma_{eff}^{pr}, \tag{63}$$

$$\Delta\gamma = \sqrt{\frac{3}{2}}\Delta\varepsilon_{eq}^{pl}, \tag{64}$$

and for the multilinear case

$$h\left(\varepsilon_{eq}^{pl}\big|_n + \Delta\varepsilon_{eq}^{pl}\right) = \sigma_{eff}\left(\varepsilon_{eq}^{pl}\right)\Big|_{n+1}, \tag{65}$$

and

$$h\left(\varepsilon_{eq}^{pl}\big|_n\right) = \sigma_{eff}\big|_n. \tag{66}$$

Making the previous substitutions into Equation (53) gives

$$\Delta\varepsilon_{eq}^{pl} = \frac{\sigma_{eff}^{pr} - \sigma_{ys}\big|_n}{3\mu + H}. \tag{67}$$

Recall the equation for pressure-dependent equivalent plastic strain, Equation (30)

$$\Delta\varepsilon_{eq}^{pl} = \frac{\sigma_{eff}^{pr} - \sigma_{ys}\left(\varepsilon_{eq}^{pl}\right)\Big|_{n+1} - 3ap^{pr}}{9Ka^2 + 3\mu}. \tag{68}$$

Substituting $a = 0$ for pressure-independent plasticity and

$$\sigma_{eff}\left(\varepsilon_{eq}^{pl}\right)\Big|_{n+1} = \sigma_{eff}\big|_n + H\Delta\varepsilon_{eq}^{pl} \tag{69}$$

for bilinear hardening results in repeating equation (67).

In a similar manner for the multilinear hardening case, substituting Equations (62) through (66) into Equation (61) and solving for $\Delta\varepsilon_{eq}^{pl}$ gives

$$\Delta\varepsilon_{eq}^{pl} = \frac{\sigma_{eff}^{pr} - \sigma_{eff}\left(\varepsilon_{eq}^{pl}\right)\Big|_{n+1} + \sigma_{eff}\big|_n - \sigma_{ys}\big|_n}{3\mu}. \tag{70}$$

For the case of pure isotropic hardening $\sigma_{eff}\big|_n = \sigma_{ys}\big|_n$, and Equation (70) can be written as

$$\Delta\varepsilon_{eq}^{pl} = \frac{\sigma_{eff}^{pr} - \sigma_{eff}\left(\varepsilon_{eq}^{pl}\right)\big|_{n+1}}{3\mu}, \tag{71}$$

which is identical to Equation (68) for pressure-independent ($a = 0$) plasticity. Therefore, adding the terms for $\sigma_{eff}\big|_n$ and $\sigma_{ys}\big|_n$ to the numerator of Equation (68) results in the proper form of the equation for $\Delta\varepsilon_{eq}^{pl}$ for pressure-dependent combined multilinear hardening, which is written in its final form as

$$\Delta\varepsilon_{eq}^{pl} = \frac{\sigma_{eff}^{pr} - \sigma_{ys}\left(\varepsilon_{eq}^{pl}\right)\big|_{n+1} + \sigma_{eff}\big|_n - \sigma_{ys}\big|_n - 3ap^{pr}}{9Ka^2 + 3\mu}. \tag{72}$$

4. Constitutive model programming

ABAQUS provides a useful user subroutine interface called UMAT that allows one to define complex or novel constitutive models that are not available with the built-in ABAQUS material models. UMAT's are written in FORTRAN code, and these FORTRAN subroutines are linked, compiled, and used by ABAQUS in the finite element analysis.

Two UMAT's were developed for this research. The first UMAT embodied a Drucker-Prager constitutive model with combined bilinear hardening. This subroutine was developed as a test case to confirm the validity of the pressure-dependent and combined hardening equations. The second UMAT embodied a Drucker-Prager constitutive model with combined multilinear hardening. This subroutine was developed for use in the low cycle fatigue metal plasticity analyses. Both subroutines were written in FORTRAN and are included in Allen (2002).

5. UMAT program verification

An axisymmetric finite element model of a notched round bar (NRB) geometry with the notch root radius, ρ, equal to 0.040 in. was created to simulate NRB tensile and low cycle fatigue tests. The NRB geometry was chosen to represent a specimen with a high hydrostatic stress influence (Allen, 2000). The NRB finite element model was composed of approximately 500 Q4 axisymmetric elements (type CAX4 in ABAQUS). Two planes of symmetry were utilized as illustrated in Figure 3. A uniform displacement was applied to the top nodes of the FEM's for the loading boundary condition.

The user defined constitutive model (UMAT) was compared to several of the ABAQUS built-in material models to test the accuracy of the elastoplastic equations and the corresponding FORTRAN code. Aluminum 2024-T851 material properties reported by Allen (2002) were used

in the NRB finite element model. The Drucker-Prager constant, a was 0 for von Mises plasticity and by trial and error was assumed to be 0.041 for pressure-dependent plasticity.

The first test case was the monotonic loading of the NRB FEM using the multilinear isotropic von Mises and multilinear isotropic Drucker-Prager built-in constitutive models in ABAQUS. For this case, $\beta = 1$ (pure isotropic hardening) for the combined multilinear hardening UMAT. The results of this test are shown in Figure 4, and clearly show that the global responses of the UMAT and the built-in ABAQUS models are identical.

The next test case was the cyclic loading of the NRB FEM using the bilinear kinematic von Mises model in ABAQUS. ABAQUS does not have a built-in model for the Drucker-Prager model with kinematic hardening or for the von Mises model with multilinear kinematic hardening. For this case, only the first and last values in the $\sigma - \varepsilon_{pl}$ data table were used with the combined multilinear hardening UMAT to simulate bilinear hardening, and $\beta = 0$ (pure kinematic hardening). The results of this test are shown in Figure 5, which once again show that the global responses of the UMAT and the built-in ABAQUS model are identical. The Drucker-Prager UMAT curve is included in Figure 5 for comparison and follows the expected trend.

The final test case was to examine the response of the combined multilinear hardening UMAT for varying β values. Cyclic finite element analyses with the NRB were conducted with $\beta = 0$, 0.5, and 1. The results from the first cycle are shown in Figure 6. The three FEM's have practically identical load-gage displacement responses until the negative loads are reached on the first unloading cycle. From this point on, the three solutions diverge in the expected manner with the $\beta = 0.5$ solution falling between the pure isotropic and pure kinematic curves.

6. References

1. ABAQUS Theory Manual, Version 5.5, Hibbit, Karlsson, and Sorensen, Inc., 1995.
2. ABAQUS Training Course Notes, "Writing User Subroutines with ABAQUS," Hibbitt, Karlsson, & Sorensen, Inc., 2001.
3. Allen, Phillip A., "Hydrostatic Stress Effects in Metal Plasticity," Master's Thesis, Tennessee Technological University, August 2000.
4. Allen, Phillip A., "Hydrostatic Stress Effects in Low Cycle Fatigue," Doctoral Dissertation, Tennessee Technological University, December 2002.
5. Aravas, N., "On the Numerical Integration of a Class of Pressure-Dependent Plasticity Models," International Journal for Numerical Methods in Engineering, Vol. 24, 1987, pp. 1395-1416.
6. Aravas, N., "Use of Pressure-Dependent Plasticity Models in ABAQUS," ABAQUS Users' Conference, Newport, Rhode Island, May 1996.
7. Bridgman, P.W., "The Effect of Hydrostatic Pressure on the Fracture of Brittle Substances," Journal of Applied Physics, Vol. 18, 1947, p. 246.
8. Drucker, D.C., and W. Prager, "Soil Mechanics and Plastic Analysis for Limit Design," Quarterly of Applied Mathematics, Volume 10, 1952, pp. 157-165.

9. Hill, R., "The Mathematical Theory of Plasticity," Clarendon Press, Oxford, 1950.

10. Ortiz, M. and E.P. Popov, "Accuracy and Stability of Integration Algorithms for Elastoplastic Constitutive Relations," International Journal for Numerical Methods in Engineering, Vol. 21, 1985, pp. 1561-1576.

11. Richmond, O., and W.A. Spitzig, "Pressure Dependence and Dilatancy of Plastic Flow," International Union of Theoretical and Applied Mechanics Conference Proceedings, 1980, pp. 377-386.

12. Spitzig, W.A., R.J. Sober, and O. Richmond, "Pressure Dependence of Yielding and Associated Volume Expansion in Tempered Martensite," ACTA Metallurgica, Volume 23, July 1975, pp. 885-893.

13. Spitzig, W.A., R.J. Sober, and O. Richmond, "The Effect of Hydrostatic Pressure on the Deformation Behavior of Maraging and HY-80 Steels and its Implications for Plasticity Theory," Metallurgical Transactions A, Volume 7A, Nov. 1976, pp. 377-386.

14. Spitzig, W.A. and O. Richmond, "The Effect of Pressure on the Flow Stress of Metals," ACTA Metallurgica, Vol. 32, No. 3, 1984, pp. 457-463.

15. Taylor, L.M. and D.P. Flanagan, "PRONTO 2D: A Two-Dimensional Transient Solid Dynamics Program," Sandia Report, SAND86-0594, UC-32, April 1998.

16. Wilson, Christopher D., "A Critical Reexamination of Classical Metal Plasticity," Journal of Applied Mechanics, Vol. 69, January 2002, pp. 63-68.

7. Figures

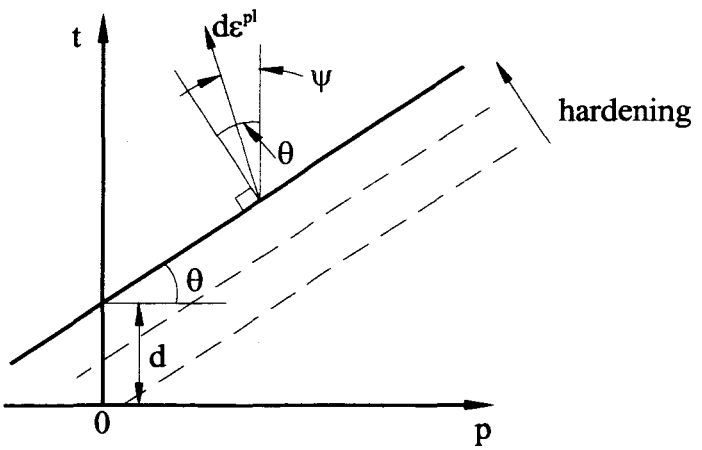

Figure 1. Linear Drucker-Prager model: yield surface and flow direction in the *p-t* plane (Adapted from (ABAQUS, 1995))

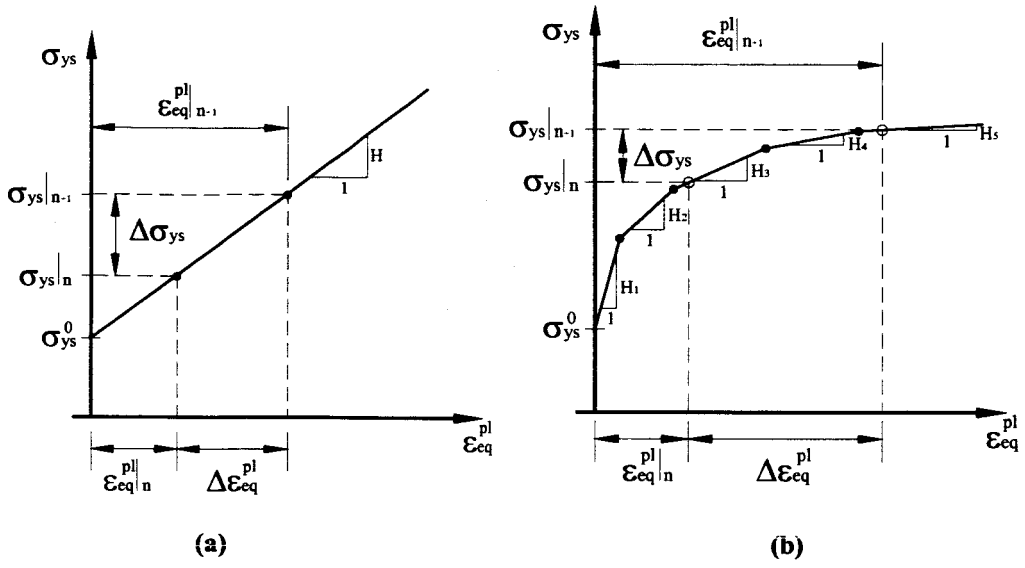

Figure 2. Illustration of the relationship between yield stress and equivalent plastic strain for the (a) bilinear hardening and (b) multilinear hardening case

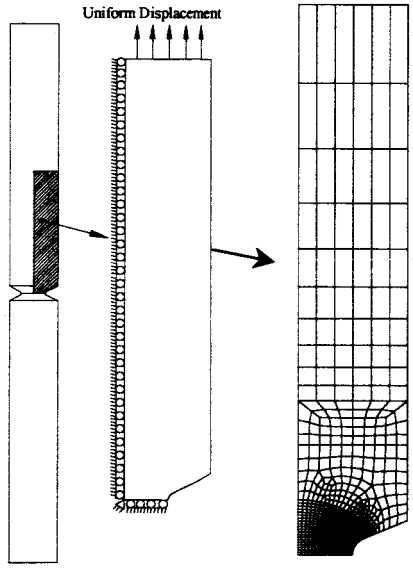

Figure 3. Schematic of axisymmetric model of a notched round bar specimen with ρ = 0.040 in. utilizing two planes of symmetry

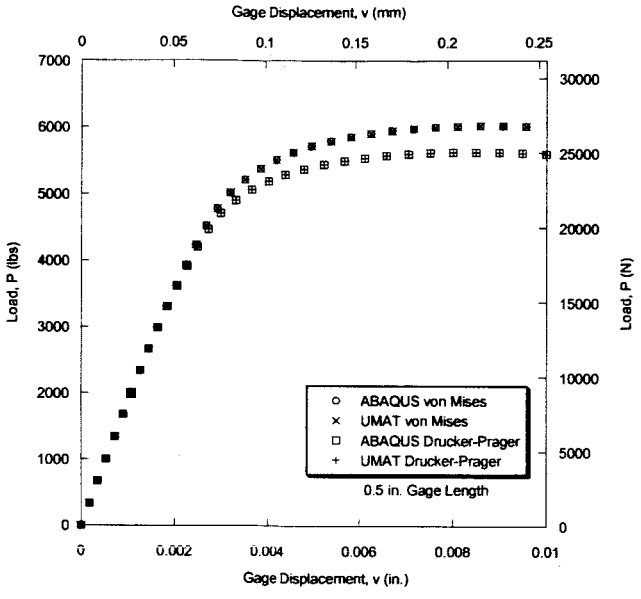

Figure 4. Comparison of the built-in ABAQUS models with multilinear isotropic hardening and the combined multilinear hardening UMAT

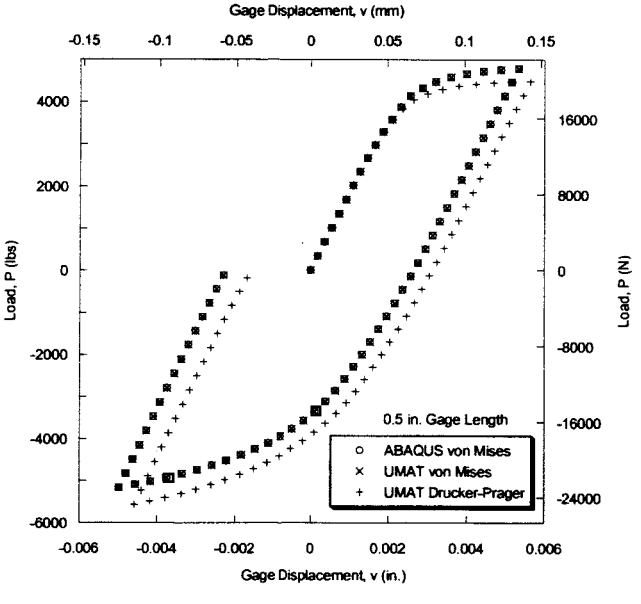

Figure 5. Comparison of the built-in ABAQUS von Mises model with bilinear kinematic hardening and the combined multilinear hardening UMAT

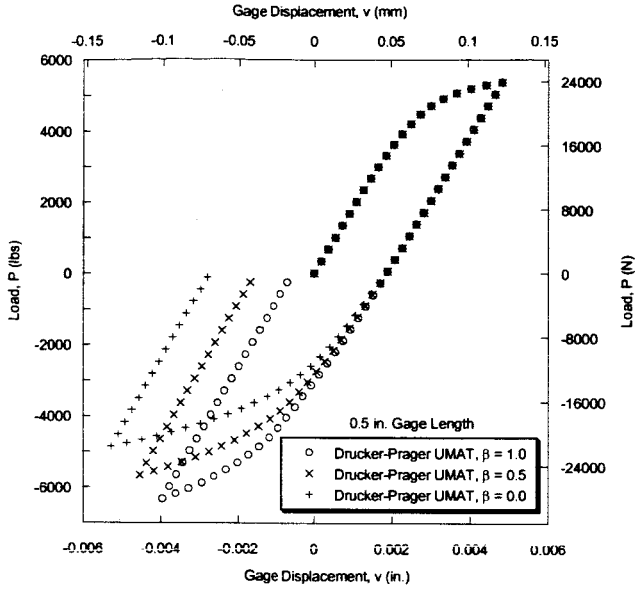

Figure 6. Comparison of Drucker-Prager combined multilinear hardening UMAT solutions with different β Values

8. Acknowledgement

We would like to thank several people at Marshall Space Flight Center for their assistance, guidance, and advice. These people include Dr. Greg Swanson, Jeff Rayburn, Dr. Preston McGill, and Doug Wells. In addition, we would like to express thanks to Bill Scherzinger and Kevin Brown at Sandia National Laboratories for their technical assistance. Funding for this research was provided by the NASA Graduate Student Researchers Program (GSRP). Support was also provided by the Center for Manufacturing Research and the Mechanical Engineering Department at Tennessee Technological University.